IEEE Access
Multidisciplinary | Rapid Review | Open Access Journal

Received May 8, 2020, accepted May 13, 2020, date of publication May 18, 2020, date of current version May 28, 2020.

Digital Object Identifier 10.1109/ACCESS.2020.2995149

CUCA Based Equivalent Fractional Order OAM Mode for Electromagnetic Vortex Imaging

SHAOQING GUO, ZI HE, (Member, IEEE), ZHENHONG FAN, AND RUSHAN CHEN, (Senior Member, IEEE)
Department of Communication Engineering, Nanjing University of Science and Technology, Nanjing 210094, China

Corresponding author: Zi He (15850554055@163.com)

This work was supported in part by the Natural Science Foundation of China under Grant 61890541, Grant 61731001, and Grant 61701232, and in part by the Jiangsu Province Natural Science Foundation of under Grant BK20170854.

ABSTRACT An equivalent fractional order orbital angular momentum (OAM) mode based on concentric uniform circular array (CUCA) is proposed in this paper. It is known that the azimuthal resolution of electromagnetic vortex imaging is closely related to the number of OAM modes. Although the multiple-in-multiple-out (MIMO) scheme gives better azimuthal resolution than the multiple-in-single-out (MISO) scheme, it suffers aliasing problem, which means the scattering points with their azimuthal difference larger than 180 degree can not be separated correctly. One possible way to solve this is adding fractional modes in MIMO scheme, but unfortunately, fractional modes are unstable and can not transmit to far field. In this paper, an equivalent fractional order OAM mode is introduced to deal with the problem to achieve higher azimuthal resolution by MIMO scheme. The transmitted and received modes are set to be two adjacent integer modes to realize an equivalent fractional mode. Since the radiation patterns generated by uniform circular array (UCA) for different modes are not aligned, concentric uniform circular array (CUCA) is applied and optimized to overcome this shortage. Simulation results demonstrate the validity of the proposed method.

INDEX TERMS Orbital angular momentum, radar imaging, fractional mode, concentric uniform circular antenna.

I. INTRODUCTION

Recently, the electromagnetic waves carrying orbital angular momentum have been applied in 2D radar staring imaging taking advantage of the dual relationship between the azimuthal angle and the OAM mode [1]–[6]. The targets can be reconstructed without relative motion with the antenna. In the past, one feasible approach to achieve staring imaging is assisted by the generation of stochastic radiation fields [7]–[9]. However, as the radiation pattern is not focus, it may not be practical for far field imaging. The electromagnetic vortex wave, with a ''doughnut'' beam, is more useful since it is focused at elevation direction.

The EM vortex wave based radar imaging has been realized using the uniform circular array (UCA). Although various methods exist to generate EM vortex wave [1]–[6], [10]–[17], the UCA is more practical for its flexibility and the ability to generate numerous OAM modes with one antenna array. Due to the orthogonality between different OAM modes, the EM vortex wave has been used in the communication system [18]–[20]. However, there are also some limitations in practical application. It is more suitable for near-field communication, or the receiving aperture needs to be very large at long distance [21]. Other researchers have studied the scattering properties from targets by different OAM modes [22]–[25]. More researches have been done in radar imaging domain. The EM vortex wave based radar imaging has been realized using the uniform circular array (UCA).

In [2], two schemes of the OAM based radar imaging were introduced including MISO scheme and MIMO scheme, and Liu pointed out that the azimuthal resolution is correlated to the range of OAM mode. Both of the two schemes can be used to achieve 2D imaging, but the MIMO scheme gives better azimuth resolution. However, it suffers aliasing problem, the scattering points with their azimuthal angle difference larger than 180 degree can not be separated correctly. To take full advantage of the higher azimuth resolution of the MIMO scheme, fractional modes should be added to increase sample

The associate editor coordinating the review of this manuscript and approving it for publication was Davide Comite.

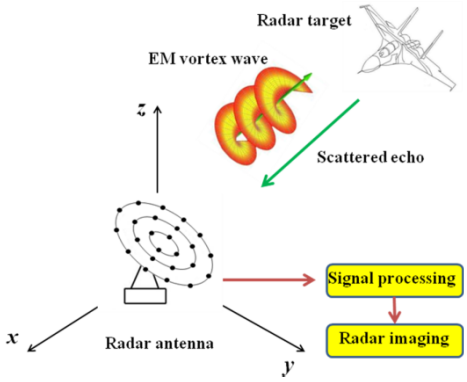

FIGURE 1. Diagram of the EM vortex wave based radar imaging system.

point in OAM domain. But unfortunately, fractional OAM modes are unstable and can not transmit to far field [26].

In this paper, an equivalent fractional order orbital angular momentum mode based on concentric uniform circular array (CUCA) [4], [5] is proposed to overcome the aliasing problem of the MIMO scheme to realize high resolution. The main lobes of different OAM modes are optimized to a same elevation angle with low side lobes. Then the transmitted and received OAM modes are set to be two adjacent integers to realize an equivalent fractional mode. The remainder of the paper is organized as follows. The aliasing problem at azimuth direction is analyzed first in Section II and then the method to realize equivalent fractional OAM mode is introduced. In section III, numerical experiments of 2D imaging are presented to verify the proposed method. A brief conclusion is given in section IV.

II. THEORY AND FORMULATION

A. ALISING PROBLEM FOR MIMO SCHEME

The sketch map of the EM vortex wave based radar imaging system is shown in Fig.1. The target can be reconstructed after processing the received echoes of multiple OAM modes.

In [2], Liu proposed two schemes to realize electromagnetic vortex imaging, the azimuth angle of the target can be reconstructed through fast Fourier transform (FFT). The normalized echoes of M ideal scattering points for MIMO mode and MISO mode α are given

$$S_{MIMO}(\alpha) = \sum_{m=1}^{M} \bar{\sigma}_m e^{i2\alpha\varphi_m} J_\alpha^2(ka\sin\theta_m) \tag{1}$$

$$S_{MISO}(\alpha) = \sum_{m=1}^{M} \bar{\sigma}_m e^{i\alpha\varphi_m} J_\alpha(ka\sin\theta_m) \tag{2}$$

where

$$\bar{\sigma}_m = \sigma_m \frac{e^{i2kr_m}}{r_m^2} \tag{3}$$

is the normalized radar cross section of the mth point, and $(r_m, \theta_m, \varphi_m)$ represents its location. Obviously, the azimuthal angle of the target can be obtained through FFT by making use of the dual relationship between the OAM mode and azimuthal angle. It is clearly that a larger range of OAM mode leads to a better azimuthal resolution. If $\alpha = -l \sim l$, the azimuthal resolution for MISO mode is

$$\rho_\varphi \approx \frac{2\pi}{\Delta\alpha} \tag{4}$$

in which $\Delta\alpha = 2l$ represents the range of OAM mode. While the azimuthal resolution for MIMO scheme is better

$$\rho_\varphi \approx \frac{\pi}{\Delta\alpha} \tag{5}$$

This can be explained in a simple way, since there is $e^{i2\alpha\varphi}$ exist in the echo of the MIMO scheme and then $2\alpha = -2l \sim 2l$, which means the equivalent range of OAM mode in FFT is two times larger than the MISO scheme. However, as the equivalent mode interval become lager, it leads to aliasing problem. The scattering points with their azimuthal difference larger than 180 degree can not be separated correctly.

The aliasing problem can be explained in another way by the correlation function of the echo from two adjacent scattering points with same elevation angle and a different azimuth angle $\Delta\varphi$. The correlation functions for MISO and MIMO schemes are

$$\begin{aligned} g_{MISO}(\Delta\varphi) &= \int_{-\infty}^{\infty} Ae^{i\alpha\varphi} J_\alpha(ka\sin\theta) Ae^{-i\alpha(\varphi+\Delta\varphi)} J_\alpha(ka\sin\theta) d\alpha \\ &\approx \sum_{\alpha=-\infty}^{\infty} Ae^{i\alpha\varphi} J_\alpha(ka\sin\theta) Ae^{-i\alpha(\varphi+\Delta\varphi)} J_\alpha(ka\sin\theta) \end{aligned} \tag{6}$$

$$\begin{aligned} g_{MIMO}(\Delta\varphi) &= \int_{-\infty}^{\infty} Ae^{i2\alpha\varphi} J_\alpha^2(ka\sin\theta) Ae^{-i2\alpha(\varphi+\Delta\varphi)} J_\alpha^2(ka\sin\theta) d\alpha \\ &\approx \sum_{\alpha=-\infty}^{\infty} Ae^{i2\alpha\varphi} J_\alpha^2(ka\sin\theta) Ae^{-i2\alpha(\varphi+\Delta\varphi)} J_\alpha^2(ka\sin\theta) \end{aligned} \tag{7}$$

in which $A = \sigma e^{i2kr}/r^2$, and for simplicity, the scattering coefficient σ=1.

The normalized correlation function is equal to 1 when the two scattering points coincide ($\Delta\varphi = 0$). And then the magnitude of the correlation function decrease when $\Delta\varphi$ is gradually increased so that the two points can just be distinguished when g($\Delta\varphi$) is small enough.

As shown in Fig.2, the normalized correlation function of MIMO scheme has a periodic of 180 degree while the MISO scheme is 360 degree which means the difference azimuthal angle of the scattering points larger than 180 degree can not be reconstructed correctly by the MIMO scheme. The scattering point with a azimuth angle of (φ + 180) may be wrongly reconstructed at φ. Although the MISO mode does not suffer the aliasing problem, its azimuthal resolution is not as good as the MIMO scheme. This also can be seen from Fig.2 that the main lobe of the MISO mode is much wider than the MIMO scheme.

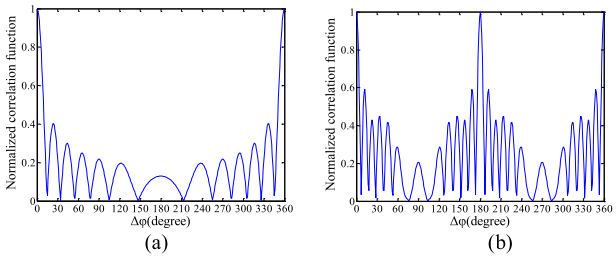

FIGURE 2. Normalized correlation functions. (a) MISO scheme, (b) MIMO scheme. The radius of UCA is a = 0.15m, the frequency is f = 6GHz, θ = 30degree.

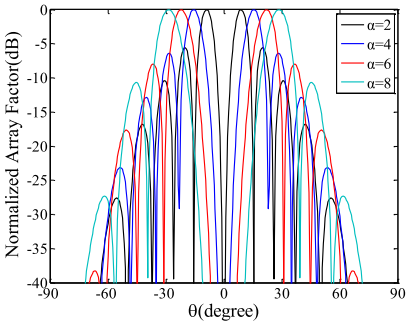

FIGURE 3. Normalized radiation patterns of φ = 0 degree for different OAM modes, the radius of UCA is a = 0.15m, the frequency is f = 6GHz.

The aliasing problem can be solved by adding fractional modes in the MIMO scheme. When fractional order OAM modes are used, for instance $\alpha = -l, -l+0.5, -l+1, \ldots, l-1, l-0.5, l$, then $2\alpha = -2l, -2l+1, -2l+2, \ldots, 2l-2, 2l-1, 2l$. Thus the equivalent sampling interval in OAM mode domain can be kept at 1. But unfortunately, fractional modes are unstable and can not transmit to far field [26]. In this paper, equivalent fractional order OAM mode is introduced in the following.

B. EQUIVALENT FRACTIONAL OAM MODE

In this section, an equivalent fractional order OAM mode is realized through a simple approach, the transmitted and received modes are set to be two different integers α and β respectively, then the echo can be represented as

$$S(\alpha) = \sum_{m=1}^{M} \bar{\sigma}_m e^{i(\alpha+\beta)\varphi_m} J_\alpha(ka\sin\theta_m) J_\beta(ka\sin\theta_m) \quad (8)$$

where α, β are the transmitted and received OAM modes. As we can see, there is $e^{i(\alpha+\beta)\varphi_m}$ in (8). Then the echo can be considered as the MIMO scheme with an equivalent mode of $(\alpha+\beta)/2$. If $\beta = \alpha+1$, the equivalent mode is $\alpha+0.5$.

However, as the main lobes of different OAM modes generated by a same UCA are not matched [4] as shown in Fig.3. The magnitude of the echo (8) maybe too small which is bad for radar imaging.

In order to collimate the beams of different OAM modes to a same elevation direction, the concentric uniform circular array (CUCA), as shown in Fig.4 was proposed in [4].

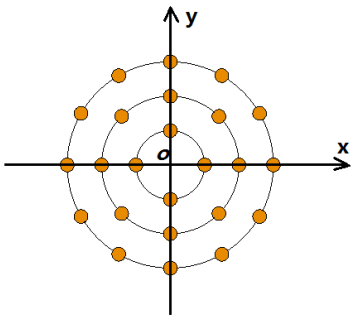

FIGURE 4. Concentric uniform circular antenna.

TABLE 1. Optimized feed amplitude for each circle.

Feed amplitude		OAM mode									
		1	2	3	4	5	6	7	8	9	10
Radius of each circle(m	$a1$=0.05	0.87	0.24	0.01	0.30	0.55	0.51	0.76	0.38	0.59	0.48
	$a2$=0.10	0.34	1	0.46	0	0	0	0.24	0.91	0.96	0.93
	$a3$=0.15	0	0.34	0.83	0.85	0.45	0.07	0	0	0.30	0.02
	$a4$=0.20	0	0	1	1	0.96	1	0.19	0.18	0.20	0.13
	$a5$=0.25	0	0	0	1	1	1	0.78	1	0.02	0
	$a6$=0.30	0	0	0	0	1	1	1	1	0.75	0.15
	$a7$=0.35	0	0	0	0	0	0.38	1	1	1	0.49
	$a8$=0.40	0	0	0	0	0	0	0.29	1	1	0.83
	$a9$=0.45	0	0	0	0	0	0	0.18	0.53	1	0.86
	$a10$=0.50	0	0	0	0	0	0	0	0	0.71	0.84

And the excitation amplitudes for each circle can be optimized to suppress the side lobe of each OAM mode [5] to improve the imaging quality.

In this paper, covariance matrix adaptation evolution strategy (CMA-ES) [27], [28] is used to collimate and optimize the beams of different OAM modes at 6GHz. CMA-ES is an adaptive algorithm which can learn from the relativity of the complex parameters. Compared with the common used genetic algorithm, this adaptive algorithm has faster optimization speed and better robustness, and is more suitable for solving the problem with large number of optimization variables.

The radius of each circle of the CUCA are listed in table 1. The designed elevation angle of the main lobe is point to θ = 11degree. And the unit radiation pattern is assumed as

$$f(\theta, \phi) = \frac{1+\cos(\pi\sin\theta)}{\cos\theta} \quad (9)$$

It should be noted that Eq. (9) can be replaced by other kind of element pattern. The optimized feed amplitudes for each circle are listed in table 1 and the optimized normalized radiation patterns of different OAM mode are shown in Fig.5. As we can seen, the main lobes of different OAM modes are almost directed to a same elevation angle of θ = 11degree, and the side-lobe level is suppressed lower than −20dB.

According to the MIMO scheme, the transmitted signal by CUCA of α mode after optimization is received by each element which can be represented as [5]

$$S_r(\alpha) = \sum_{m=1}^{M} \bar{\sigma}_m \frac{e^{-i2kr_m}}{r_m^2} e^{i\alpha\varphi_m} \sum_{h=1}^{H} I_h J_\alpha(ka_h\sin\theta_m) \quad (10)$$

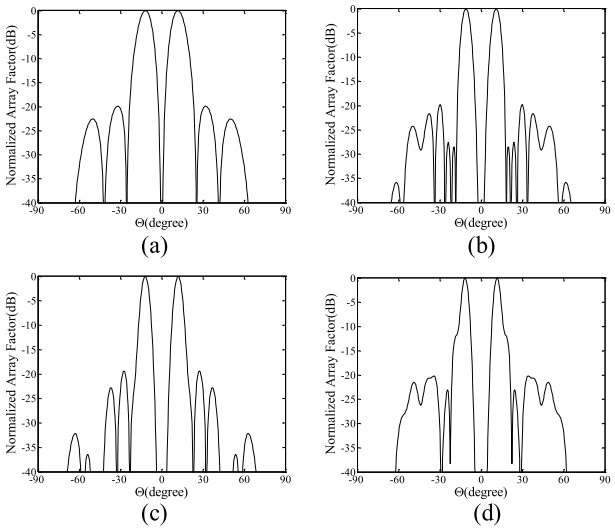

FIGURE 5. Radiation patterns of different OAM mode. (a) $\alpha = 2$, (b) $\alpha = 4$, (c) $\alpha = 6$, (d) $\alpha = 8$.

in which I_h is the feed amplitude of the hth circle. When the received mode is β, which means the received signal of the nth array element is multiplied by the phase of $e^{i\beta\phi_n}$, the final echo can be represented as

$$S_r(\alpha, \beta) = AB \sum_{m=1}^{M} \bar{\sigma}_m \frac{e^{-i2kr_m}}{r_m^2} e^{i(\alpha+\beta)\varphi_m} \tag{11}$$

in which

$$A = \sum_{h=1}^{H} I_h J_\alpha(ka_h \sin\theta_m) \tag{12}$$

$$B = \sum_{h=1}^{H} I_h J_\beta(ka_h \sin\theta_m) \tag{13}$$

In this paper, the received mode is set as $\beta = \alpha+1$. The transmitted OAM modes are $-10\sim10$. The equivalent fractional modes are $-9.5\sim9.5$. Then 2D imaging can be achieved through fast Fourier transform.

III. SIMULATION IMAGING RESULTS

In this section, numerical experiments are conducted to verify the proposed method. Firstly, 1-D imaging is realized at single frequency, assume that two scattering points are located at a same distance and a same elevation angle but different azimuth angle. For case1, the difference of the azimuth angle is less than 180 degree, while for case2 the difference is larger than 180 degree as shown in table 2. The full range of the OAM mode is $\Delta\alpha = -10, -9.5, -9, \ldots 9, 9.5, 10$, and the frequency is fixed at 6GHz. The optimized parameters of the CUCA are given in table 1.

The imaging results are shown in Fig.6, for case 1, as we can see, the azimuth angle of the two points can be reconstructed correctly when their difference is less than 180 degree. While for case2, the scattering points can not

TABLE 2. Locations of the two scattering points in the first experiment.

scattering points	$P_1(r_1, \theta_1, \varphi_1)$	$P_2(r_1, \theta_1, \varphi_1)$
case1	(1000m, 11°, 54°)	(1000m, 11°, 90°)
case2	(1000m, 11°, 54°)	(1000m, 11°, 270°)

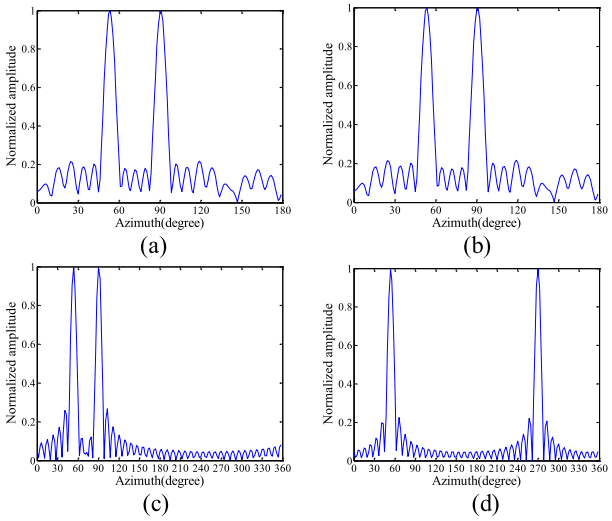

FIGURE 6. 1-D imaging results of two scattering points. (a) only integer modes for case1, (b) integer modes and fractional modes for case1, (c) only integer modes for case2, (d) integer modes and fractional modes for case2.

TABLE 3. Locations of the two scattering points in the second experiment.

scattering points	$P_1(r_1, \theta_1, \varphi_1)$	$P_2(r_1, \theta_1, \varphi_1)$
case1	(1000m, 11°, 50°)	(1000m, 11°, 245°)
case2	(1000m, 11°, 50°)	(1000m, 11°, 65°)

be reconstructed correctly if only integer modes are applied. The equivalent fractional OAM mode is feasible to handle this problem.

Secondly, the resolution of the two schemes are compared by another 1-D imaging experiment. The frequency is fixed at 6GHz, and for MISO scheme, the OAM mode applied in the experiment is $-10\sim10$ but only the integer part, while for MIMO scheme the OAM mode is the same as the first experiment. The two scattering points are with a same distance and same elevation angle but different azimuth angle similar to the first experiment, and the two scattering points used here are much closer in the azimuth direction as shown in table 3.

The imaging results are shown in Fig.7. For case 1, as we can see, both of the two schemes can reconstruct the azimuth angles of the two points correctly, demonstrating that the MISO scheme doesn't suffer the aliasing problem. However, for case 2, the two scattering points cannot be separated through the MISO scheme since the resolution of the MIMO scheme is better than the MISO scheme.

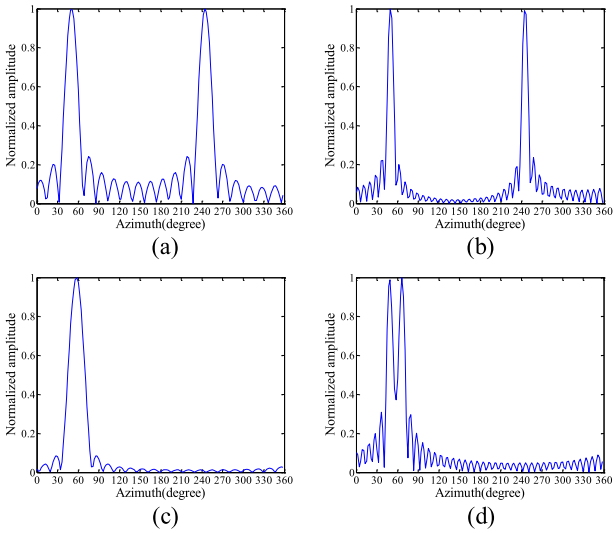

FIGURE 7. 1-D imaging results of two scattering points. (a) MISO scheme for case1, (b) MIMO scheme with integer modes and fractional modes for case1, (c) MISO scheme for case2, (d) MIMO scheme with integer modes and fractional modes for case2.

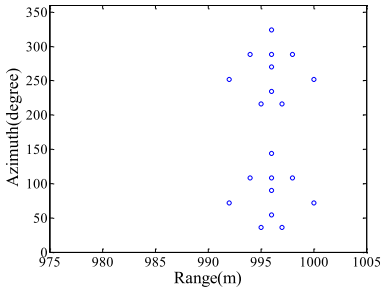

FIGURE 8. Two "plane" model consist of 20 scattering points.

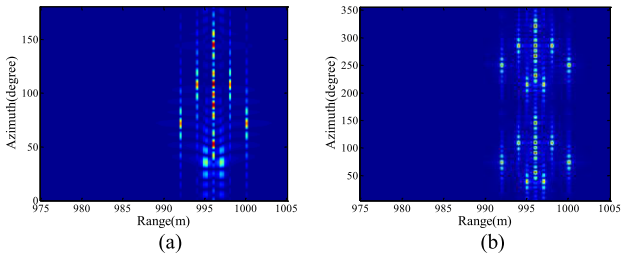

FIGURE 9. 2-D Imaging results of two "plane" model consist of 20 scattering points. (a) only integer modes, (b) integer modes and fractional modes.

In the third experiment, the capability of the 2-D EM vortex imaging is verified, two "plane" model consist of 20 scattering points is shown in Fig.8. The different azimuth angle of the two "plane" is 180 degree. The range of OAM mode applied here is the same as the first experiment, the center frequency is 6GHz with a frequency bandwidth of 500MHz.

The imaging results are shown in Fig.9. The two "plane" can be reconstructed correctly with the equivalent fractional OAM mode. While by the traditional MIMO scheme with only integer modes, only one "plane" appears in the imaging result.

IV. CONCLUSION

The OAM based radar imaging method is a new computational imaging scheme, targets can be reconstructed by applying multiple OAM modes and the computation of the echo without relative motion. In this paper, an equivalent fractional OAM mode is proposed for the first time to solve the aliasing problem in MIMO scheme to realize high resolution in EM vortex radar imaging. The transmitted and received OAM modes are set as two adjacent integers to achieve an equivalent fractional mode. Considering different modes of the EM vortex wave generated by one single UCA radiate to different elevation angle, the optimized CUCA is used to collimate the radiation patterns of different modes to a same angle with low side-lobes. Then 1D and 2D imaging based on MIMO mode is realized through FFT, simulation results validate the effectiveness of the proposed method.

REFERENCES

[1] G. R. Guo, W. Hu, and X. Du, "Electromagnetic vortex based radar target imaging," *J. Nat. Univ. Defense Technol.*, vol. 35, no. 6, pp. 71–76, Dec. 2013.
[2] K. Liu, Y. Cheng, Z. Yang, H. Wang, Y. Qin, and X. Li, "Orbital-angular-momentum-based electromagnetic vortex imaging," *IEEE Antennas Wireless Propag. Lett.*, vol. 14, pp. 711–714, 2015.
[3] K. Liu, H. Liu, Y. Qin, Y. Cheng, S. Wang, X. Li, and H. Wang, "Generation of OAM beams using phased array in the microwave band," *IEEE Trans. Antennas Propag.*, vol. 64, no. 9, pp. 3850–3857, Sep. 2016.
[4] T. Yuan, H. Wang, Y. Qin, and Y. Cheng, "Electromagnetic vortex imaging using uniform concentric circular arrays," *IEEE Antennas Wireless Propag. Lett.*, vol. 15, pp. 1024–1027, 2016.
[5] Y. Qin, K. Liu, Y. Cheng, X. Li, H. Wang, and Y. Gao, "Sidelobe suppression and beam collimation in the generation of vortex electromagnetic waves for radar imaging," *IEEE Antennas Wireless Propag. Lett.*, vol. 16, pp. 1289–1292, 2017.
[6] S. Guo, Z. He, and R. Chen, "High resolution 2-D electromagnetic vortex imaging using uniform circular arrays," *IEEE Access*, vol. 7, pp. 132430–132437, 2019.
[7] Y. Guo, D. Wang, X. He, and B. Liu, "Super-resolution staring imaging radar based on stochastic radiation fields," in *IEEE MTT-S Int. Microw. Symp. Dig.*, Nanjing, China, Sep. 2012, pp. 1–4.
[8] C. Tian, Z. Jiang, W. Chen, and D. Wang, "Adaptive microwave staring correlated imaging for targets appearing in discrete clusters," *Sensors*, vol. 17, no. 10, p. 2409, 2017.
[9] H. Yang, L. Zhang, Y. Gao, K. Wang, and X. Liu, "Azimuth wavefront modulation using plasma lens array for microwave staring imaging," in *Proc. IEEE Int. Geosci. Remote Sens. Symp. (IGARSS)*, Milan, Italy, Jul. 2015, pp. 4276–4279.
[10] M. L. N. Chen, L. J. Jiang, and W. E. I. Sha, "Quasi-continuous metasurfaces for orbital angular momentum generation," *IEEE Antennas Wireless Propag. Lett.*, vol. 18, no. 3, pp. 477–481, Mar. 2019.
[11] M. L. N. Chen, L. J. Jiang, and W. E. I. Sha, "Generation of orbital angular momentum by a point defect in photonic crystals," *Phys. Rev. A, Gen. Phys.pplied*, vol. 10, no. 1, Jul. 2018, Art. no. 014034.
[12] S. Yu, L. Li, G. Shi, C. Zhu, X. Zhou, and Y. Shi, "Design, fabrication, and measurement of reflective metasurface for orbital angular momentum vortex wave in radio frequency domain," *Appl. Phys. Lett.*, vol. 108, no. 12, Mar. 2016, Art. no. 121903.
[13] S. Yu, L. Li, and N. Kou, "Generation, reception and separation of mixed-state orbital angular momentum vortex beams using metasurfaces," *Opt. Mater. Express*, vol. 7, no. 9, pp. 3312–3321, Sep. 2017.
[14] F. Shen, J. Mu, K. Guo, S. Wang, and Z. Guo, "Generation of continuously variable-mode vortex electromagnetic waves with three-dimensional helical antenna," *IEEE Antennas Wireless Propag. Lett.*, vol. 18, no. 6, pp. 1091–1095, Jun. 2019.

[15] Z. Chang, B. You, L.-S. Wu, M. Tang, Y.-P. Zhang, and J.-F. Mao, "A reconfigurable graphene reflectarray for generation of vortex THz waves," *IEEE Antennas Wireless Propag. Lett.*, vol. 15, pp. 1537–1540, 2016.
[16] S. Zheng, X. Hui, X. Jin, H. Chi, and X. Zhang, "Transmission characteristics of a twisted radio wave based on circular traveling-wave antenna," *IEEE Trans. Antennas Propag.*, vol. 63, no. 4, pp. 1530–1536, Apr. 2015.
[17] Z. Zhang, S. Zheng, X. Jin, H. Chi, and X. Zhang, "Generation of plane spiral OAM waves using traveling-wave circular slot antenna," *IEEE Antennas Wireless Propag. Lett.*, vol. 16, pp. 8–11, 2017.
[18] Y. Yang, W. Cheng, W. Zhang, and H. Zhang, "Mode modulation for wireless communications with a twist," *IEEE Trans. Veh. Technol.*, vol. 67, no. 11, pp. 10704–10714, Nov. 2018.
[19] B. Allen, A. Tennant, E. Chatziantoniou, and Q. Bai, "Wireless data encoding and decoding using OAM modes," *Electron. Lett.*, vol. 50, no. 3, pp. 232–233, Jan. 2014.
[20] E. Cano and B. Allen, "Multiple-antenna phase-gradient detection for OAM radio communications," *Electron. Lett.*, vol. 51, no. 9, pp. 724–725, Apr. 2015.
[21] A. F. Morabito, L. Di Donato, and T. Isernia, "Orbital angular momentum antennas: Understanding actual possibilities through the aperture antennas theory," *IEEE Antennas Propag. Mag.*, vol. 60, no. 2, pp. 59–67, Apr. 2018.
[22] C. Zhang, D. Chen, and X. Jiang, "RCS diversity of electromagnetic wave carrying orbital angular momentum," *Sci. Rep.*, vol. 7, no. 1, Dec. 2017, Art. no. 15412.
[23] M. P. Yu, Y. Han, and Z. Cui, "Scattering of non-diffracting vortex electromagnetic wave by typical targets," *Prog. Electromagn. Res. Lett.*, vol. 70, pp. 139–146, 2017.
[24] T. Bo, B. Jian, and S. Xin-Qing, "Orbital-angular-momentum-carrying wave scattering by the chaff clouds," *IET Radar, Sonar Navigat.*, vol. 12, no. 6, pp. 649–653, Mar. 2018.
[25] C. Zhang and D. Chen, "Large-scale orbital angular momentum radar pulse generation with rotational antenna," *IEEE Antennas Wireless Propag. Lett.*, vol. 16, pp. 2316–2319, 2017.
[26] P. Ding, "Stabilization analysis of phase singularity of vortex beams with integral and fractional orders," (in Chinese), *J. Huazhong Univ. Sci. Technol. (Natural Sci. Ed.)*, vol. 39, no. 5, pp. 118–122, 2011.
[27] N. Hansen and A. Ostermeier, "Completely derandomized self-adaptation in evolution strategies," *Evol. Comput.*, vol. 9, no. 2, pp. 159–195, Jun. 2001.
[28] A. Auger and N. Hansen, "A restart CMA evolution strategy with increasing population size," in *Proc. IEEE Congr. Evol. Comput.*, Edinburgh, Scotland, vol. 2, Sep. 2005, pp. 1769–1776.

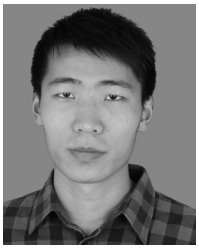

SHAOQING GUO was born in Hebei, China. He received the B.Sc. degree in detection, guidance, and control technology from the School of Electrical Engineering and Optical Technique, Nanjing University of Science and Technology, Nanjing, China, in 2013, where he is currently pursuing the Ph.D. degree in electromagnetic fields and microwave technology. His research interests include computational electromagnetics, radar signal processing, electromagnetic vortex wave, radar target detection, and imaging.

ZI HE (Member, IEEE) was born in Hebei, China. She received the B.Sc. and Ph.D. degrees in electronic information engineering from the School of Electrical Engineering and Optical Technique, Nanjing University of Science and Technology, Nanjing, China, in 2011 and 2016, respectively.

She has worked as a Visiting Scholar at the University of Illinois at Urbana–Champaign (UIUC), from September 2015 to September 2016. She works as a Postdoctoral Researcher with the Science and Technology on Electromagnetic Scattering Laboratory, BIEF. Since 2016, she has been an Assistant Professor with the Department of Communication Engineering, Nanjing University of Science and Technology. Her research interests include antenna, RF-integrated circuits, and computational electromagnetics.

ZHENHONG FAN was born in Jiangsu, China, in 1978. He received the M.Sc. and Ph.D. degrees in electromagnetic field and microwave technique from the Nanjing University of Science and Technology (NJUST), Nanjing, China, in 2003 and 2007, respectively. In 2006, he was a Research Assistant with the Center of wireless Communication, City University of Hong Kong. He is currently a Professor of electronic engineering with NJUST. He is the author or a coauthor of over 50 technical articles. His current research interests include computational electromagnetics and electromagnetic scattering and radiation.

RUSHAN CHEN (Senior Member, IEEE) was born in Jiangsu, China. He received the B.Sc. and M.Sc. degrees from the Department of Radio Engineering, Southeast University, China, in 1987 and 1990, respectively, and the Ph.D. degree from the Department of Electronic Engineering, City University of Hong Kong, in 2001.

He joined the Department of Electrical Engineering, Nanjing University of Science and Technology (NJUST), China, where he became a Teaching Assistant, in 1990, and a Lecturer, in 1992. Since September 1996, he has been a Visiting Scholar with the Department of Electronic Engineering, City University of Hong Kong, as a Research Associate, a Senior Research Associate, in July 1997, a Research Fellow, in April 1998, and a Senior Research Fellow, in 1999. From June to September 1999, he was also a Visiting Scholar with the University of Montreal, Canada. In September 1999, he was promoted to a Full Professor and an Associate Director of the Microwave and Communication Research Center, NJUST. In 2007, he was appointed as the Head of the Department of Communication Engineering, NJUST. He was appointed as the Dean of the School of Communication and Information Engineering, Nanjing Post and Communications University, in 2009. In 2011, he was appointed as the Vice Dean of the School of Electrical Engineering and Optical Technique, NJUST. He is currently a Principal Investigator of more than ten national projects. He has authored or coauthored more than 260 articles, including over 180 articles in international journals. His research interests mainly include computational electromagnetics, microwave integrated circuit and nonlinear theory, smart antenna in communications and radar engineering, microwave material and measurement, RF-integrated circuits, and so on.